



Bioactivity Behavior of Nano-hydroxyapatite Filled Chitosan / Polyacrylamide Composite

A. M. Abdelghany^{1*}, M. Meikhail², S.I. Badr², D. A. Agag².

1. Spectroscopy Department, Physics Division, National Research Center, ET- 12311, Giza, Egypt

2. Physics Department, Faculty of Science, Mansoura University, ET- 35516, Mansoura, Egypt

ABSTRACT

Chitosan/Polyacrylamide containing nano-hydroxyapatite (HA) composite were prepared via in situ preparation technique. XRD (x-ray diffraction), (FTIR) Fourier transform infrared spectroscopy, (TEM) transmission electron microscopy, (SEM) scanning electron microscopy and (DSC) differential scanning calorimetry were used to characterize the prepared nano-composites before and after immersion in simulated body fluid (SBF). XRD confirm that addition of hydroxyapatite (HA) in the filling level has no effect on the amorphous nature of the base polymeric material with minor change in their crystallinity. FTIR spectra shows maintenance of the basic vibrational band corresponding to chitosan (CHI) and polyacrylamide (PAAm), while the change in the intensity of the peaks at 1092 and 1043 cm^{-1} indicates interaction between inorganic and organic matrix. Scanning electron micrographs of prepared samples before and after immersion in (SBF) shows a formation of crystalline regions of HA which confirmed by EDX measurements.

Keywords: Chitosan/Polyacrylamide blend; nano-Hydroxyapatite; SBF; FTIR; XRD.

*Corresponding Author Email a.m_abdelghany@yahoo.com

Received 17 May 2014, Accepted 29 May 2014

INTRODUCTION

In recent years, significant research effort has been devoted to developing inorganic nanocrystals because of their potential application in biology, electronics, optics, transportation, and information technology. Although several approaches investigated ways of making these nanocrystals, controlling the size, shape and crystallinity and various parameters affecting the size and shape of these materials still need to be found¹.

Bionanocomposites form a fascinating interdisciplinary area that brings together biology, materials science, and nanotechnology. New bionanocomposites are impacting diverse areas, in particular, biomedical science. Generally, polymer nanocomposites are the result of the combination of polymers and inorganic/organic fillers at the nanometer scale. The extraordinary versatility of these new materials springs from the large selection of biopolymers and fillers available to researchers. Existing biopolymers include, but are not limited to, polysaccharides, aliphatic polyesters, polypeptides and proteins, and polynucleic acids, whereas fillers include clays, hydroxyapatite, and metal nanoparticles. The interaction between filler components of nanocomposites at the nanometer scale enables them to act as molecular bridges in the polymer matrix. This is the basis for enhanced mechanical properties of the nanocomposite as compared to conventional micro composites. Bionanocomposites add a new dimension to these enhanced properties in that they are biocompatible and/or biodegradable materials².

Hydroxyapatite (HA), $\text{Ca}_{10}(\text{PO}_4)_6(\text{OH})_2$, is one of the major constituents of the inorganic components in human hard tissues (bones and teeth) and thus it is one of the most biocompatible materials. The chemical species constituting HA crystals (Ca, P, O and H) are expected to have no toxicity. It is also a promising material as reinforcing filler for composites, insulating agents and chromatomedium for simple, rapid fraction of proteins and nucleic acids³. Hydroxyapatite belongs to the apatite family. Apatite is the name given to a group of crystals of the general chemical formula $\text{M}_{10}(\text{XO}_4)_6\text{Z}_2$, where $\text{M} = \text{Ca}^{2+}, \text{Sr}^{2+}, \text{Ba}^{2+}, \text{Na}^+, \text{Pb}^{2+}, \text{La}^{3+}$, and many rare earth elements; $\text{XO}_4 = \text{PO}_4^{3-}, \text{VO}_4^{3-}, \text{SiO}_4^{4-}, \text{AsO}_4^{3-}, \text{CO}_3^{2-}$; $\text{Z} = \text{OH}^-, \text{Cl}^-, \text{F}^-, \text{CO}_3^{2-}$. The molar ratio of calcium to phosphorus Ca/P varies from 1.2 to almost 2 in HA. The stoichiometric molar ratio of HA is 1.67; however, this is not the value observed in the organism because small amounts of other materials such as carbon, nitrogen, iron and other elements are incorporated. This biomaterial is widely used to repair, fill, extend and reconstruct damaged bone tissue. It can also be used in soft tissue. Hydroxyapatite can be manufactured synthetically by using a number of different methods. The processes for the preparation of hydroxyapatite and any other calcium

phosphate powders may be classified under two main headings: synthesis from mammal bones or coral and in the lab, in this case it can be synthesized by reactions in solid state, coprecipitation, hydrothermal methods, sol-gel process, microwave processing, among others. The most popular methods are chemical coprecipitation from water solutions containing the ions Ca^{2+} , PO_4^{3-} , and OH^- , which in conditions of $\text{pH} > 7$, form primary crystallites of insoluble hydroxyapatite ⁴.

Many researchers have previously tried different combinations of polyacrylamide (PAAm) and chitosan (CHI) by either grafting or blending them with each other. Polyacrylamide forms good blends with chitosan ⁵.

The main aim of the present work is to use nano hydroxyapatite as filler for PAAm/CHI polymer blend to highlight the effects of the polymeric matrix on the biophysical properties, for biological applications. Also, to investigate the bioactivity of the nanohydroxyapatite / polymer blend composites using simulated body fluid (SBF).

MATERIALS AND METHOD

Chemicals Materials

Calcium nitrate A.R [$\text{Ca}(\text{NO}_3)_2 \cdot 4\text{H}_2\text{O}$] from WINLAB, UK, diammonium hydrogen phosphate [$(\text{NH}_4)_2\text{HPO}_4$] from Sisco research laboratories PVT. LTD, India. Ammonium Hydroxide [NH_4OH], Polyacrylamide (PAAm) was purchased from the chemical agent supplier of Shanghai, whose average molecular weight (Mw) was 5.0×10^6 . Deionized water, Chitosan [2-Amino-2-deoxy-(1-4) glucopyranan] from Fluka Mr 600000.

Preparation of nanohydroxyapatite chitosan / polyacrylamide composite

$\text{Ca}(\text{NO}_3)_2 \cdot 4\text{H}_2\text{O}$ and $(\text{NH}_4)_2\text{HPO}_4$ were dissolved in deionized water separately. The pH of each aqueous solution was adjusted to 11 using NH_4OH solution 25%. The drop wise addition of $\text{Ca}(\text{NO}_3)_2$ aqueous solution to vigorously stirred $(\text{NH}_4)_2\text{HPO}_4$ solution at room temperature for about 1h produced a milky and somewhat gelatinous precipitate which was then stirred for 1h. After washing and filtering the precipitate was dried at 100°C overnight and calcined in alumina crucible at 1000°C for 2h.

Formation of nano hydroxyapatite follows the following equation:



Equimass fractions of both PAAm and CHI were added to prepare base polymer blend. Calculated mass fractions of HA filler were added according to table (1).

Table 1: Sample composition:

Sample	CHI	PAAm	HA
S ₀	50.0	50.0	0.0
S ₁	49.5	49.5	1.0
S ₂	49.0	49.0	2.0
S ₃	47.5	47.5	5.0
S ₄	40.0	40.0	10
S ₅	100	0.0	0.0
S ₆	0.0	100	0.0
S ₇	0.0	0.0	100

Prepare filled polymer with specified filler concentration. The filler concentration was X = 1, 2, 5 and 10.

Instrumental analysis

FT-IR absorption spectra were carried out using the single beam Fourier transform-infrared spectrometer (Nicolet iS10, USA) in the spectral range of 400 – 4000 cm⁻¹. X-ray diffraction scans were obtained using PANalytical X'Pert PRO XRD system using CuK_α radiation (where, $\lambda = 1.540 \text{ \AA}$, the tube operated at 30 kV, the Bragg's angle (2θ) in the range of 4-50°). Differential scanning calorimetry (DSC) of the prepared films was conducted using an instrument type (SDT Q600 V20.5 Build 15). Briefly, 15-25 mg from the sample is heating from room temperature to 500 °C with a heating rate of 10 °C/min in an aluminum ban. Scanning electron micrograph of the studied samples was performed using SEM Model (Quanta 250 FEG, FEI Company, Netherlands), operating voltage at 30KV accelerating voltage. Surface of the samples were coated with 3.5 nm layer of gold to minimize sample charging effects due to the electron beam. Transmission electron microscope (TEM), (JEOL-JEM-1011, Japan) was used to study the size, shape and distribution of the nanoparticles within the polymeric matrix during preparation process.

Bioactivity measurements

FTIR and scanning electron microscopy were used as an indicator for the bioactivity of the prepared composite.

Samples of different composition were subject for measurements before and after immersion in SBF for seven days.

RESULTS AND DISCUSSION

Fourier transform infrared spectroscopy (FTIR)

Figure.1 shows FTIR absorption spectra of prepared nano hydroxyapatite. All characteristic peaks of HA supported that the Ca and P precursors were completely reacted and derived HA

without any extraneous substitution. In the middle infrared region, HA nanocrystals displayed all the peaks pertaining to hydroxyl (OH) and phosphate (PO₄) functional groups.

The characteristic peaks listed in table.2 exhibited in the sample spectra assigned here:

(a) two peaks belong to hydroxyl group, sharp peak of the stretching mode of the lattice hydrogen bonded (OH⁻) ions at 3572 cm⁻¹ and medium sharp peak for O-H bending deformation mode.

(b) There are four vibrational modes present for phosphate ions, ν_1 , ν_2 , ν_3 and ν_4 . The symmetrical stretching modes (ν_1 & ν_2) of P-O in PO₄⁻³ ions were found at 962 and 470.4 cm⁻¹, respectively, the asymmetric stretching mode (ν_3) of PO₄⁻³ ions detected at 1092 and 1043 cm⁻¹ and the bending modes (ν_4) of O-P-O have three sites observed at 633, 602 and 570 cm⁻¹ and these are well-defined and sharp peaks.

There are very small peaks at 1629 and 1465 cm⁻¹ due to the vibrational (ν_3) of carbonates (CO₃⁻²) ions. This might have originated through the absorption of carbon dioxide from the air atmosphere during processing and also a broad weak band at 3455 and 1661 cm⁻¹ due to O-H plane bending mode, assigned to the crystallization water, i.e. water molecules trapped in apatite unit cell. The presence of these peaks with very low intensity indicate that there were no formation of calcium carbonate or calcium oxide in the apatite and hence suggesting that the reaction ingredients were react well and produced phase pure n-HA.

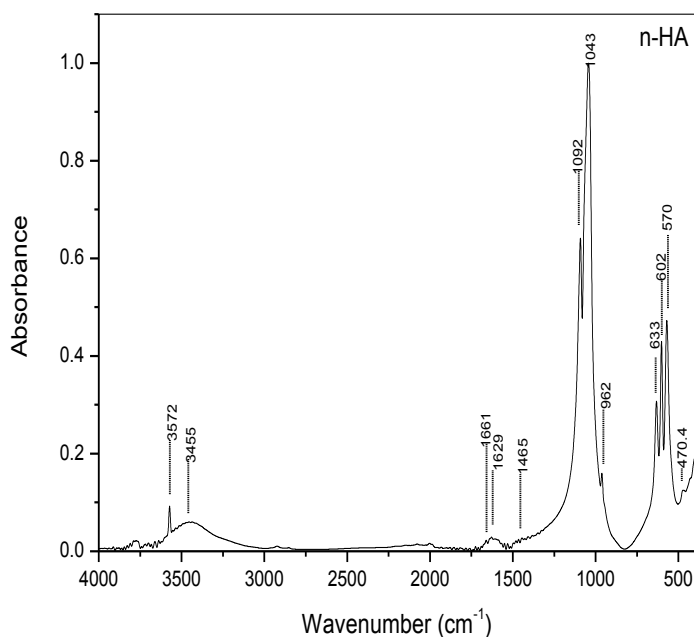


Figure.1. FTIR spectra of nanohydroxyapatite

Table 2: Infrared assigned for the synthesized hydroxyapatite powder:

Vibrational frequency(cm^{-1})	Band assignment	Reference
470.4	The symmetrical stretching modes (ν_2) of PO_4^{3-} ion	[6]
570-602	O–P–O bending	[7]
633	O–H band bending deformation mode	[8]
962	P–O symmetric stretching bonds	[3,7]
1043-1092	P–O asymmetric stretching	[3,7]
1629-1465	ν_3 vibrational modes of carbonates CO_3^{2-} ions	[1,9]
1661	O–H in-plane bending	[7]
3455	O–H stretching	[7]
3572	bulk OH^- ions	[7]

The FTIR spectra of pure chitosan, pure polyacrylamide and polymer blend (50%/50%) was presented in Figure. 2. For the pure chitosan, the strong absorption band centered at 3000-3500 cm^{-1} is concerned with the stretching vibration of N-H and O-H^{10,11} and asymmetric stretching vibration of aliphatic C-H at 2927-2880 cm^{-1} ^{10,12}, while the peaks at 1665, 1563, 1324 and 1080 cm^{-1} is due to C=O bond stretching, amide II, amide III and C–O–C stretching vibration of saccharide structure, respectively^{10,13,14}.

And the characteristic spectra for the pure PAAm was shown that a broad band around 3400 cm^{-1} due to the stretching vibration of N–H¹⁵. The significant characteristic peaks at 1670 and 1620 cm^{-1} were attributed to the carbonyl stretching vibration (amide I) and N–H bending vibration (amide II) of the amide group, respectively^{10,15} and the absorption peak at 2936 cm^{-1} was assigned to the C-H stretching vibration^{16,17}, while CH bending was detected at 1500 – 1300 cm^{-1} ¹⁶.

The FTIR spectrum of CHI-PAAm blend showed absorption bands typical to the pure components. The spectrum showed a broad absorption band around 3370 cm^{-1} due to –OH stretching of CHI and amide group of PAAm, while the peaks at 1029, 1080, 1158 and 1563 cm^{-1} in the FT-IR spectrum of chitosan are of quite reduced intensity and broad, reduced intensity of these peaks with respect to chitosan show that there is interaction between CHI and PAAm.

Figure.3 shows FT-IR absorption spectra of pure hydroxyapatite and pure blend without and with different concentrations of (1, 2, 5 and 10 wt %) hydroxyapatite. From the spectra of the composites, it shows increase in the intensity of the bands at 1092 and 1043 cm^{-1} , this increase indicates that there is interaction between the pure blend and hydroxyapatite. It can be also, observed that the band at 1563 cm^{-1} in blend become weaker with increasing HA content and it almost disappeared when 10% HA was added. The above change in this band with increasing HA content were probably due to the gradual binding between the Ca^{2+} ions of HA and the

NH₂ groups of blend indicating that good miscibility between blend and HA could be obtained at different weight ratios.

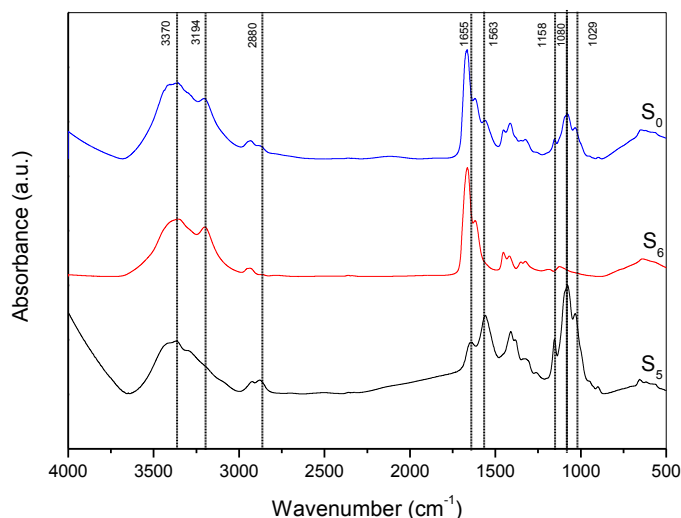


Figure. 2. FTIR spectra of pure chitosan (S₅), pure polyacrylamide (S₆) and pure polymer blend (50%/50%) (S₀)

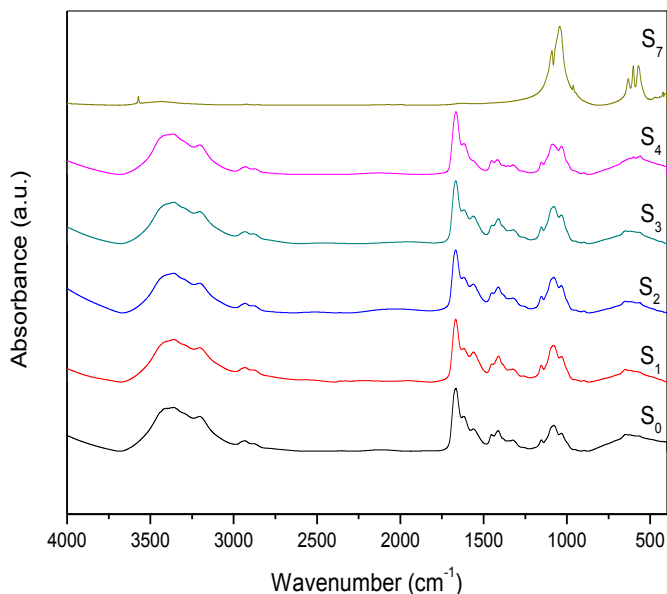


Figure.3. FTIR spectra of pure HA and pure blend without and with different concentrations of (1, 2, 5 and 10 wt %) hydroxyapatite.

The spectrum in figure.4 shows the FTIR of HA samples before and after immersion for seven days in SBF. The intensity of HA bands increased after immersion indicating that CHI-PAAM polymeric matrix increased the bioactivity of HA due to enhancement of ions deposition on the composite surface. Also, this intensity increased by increasing the concentration of HA which mean that the bioactivity improved by increasing HA concentration.

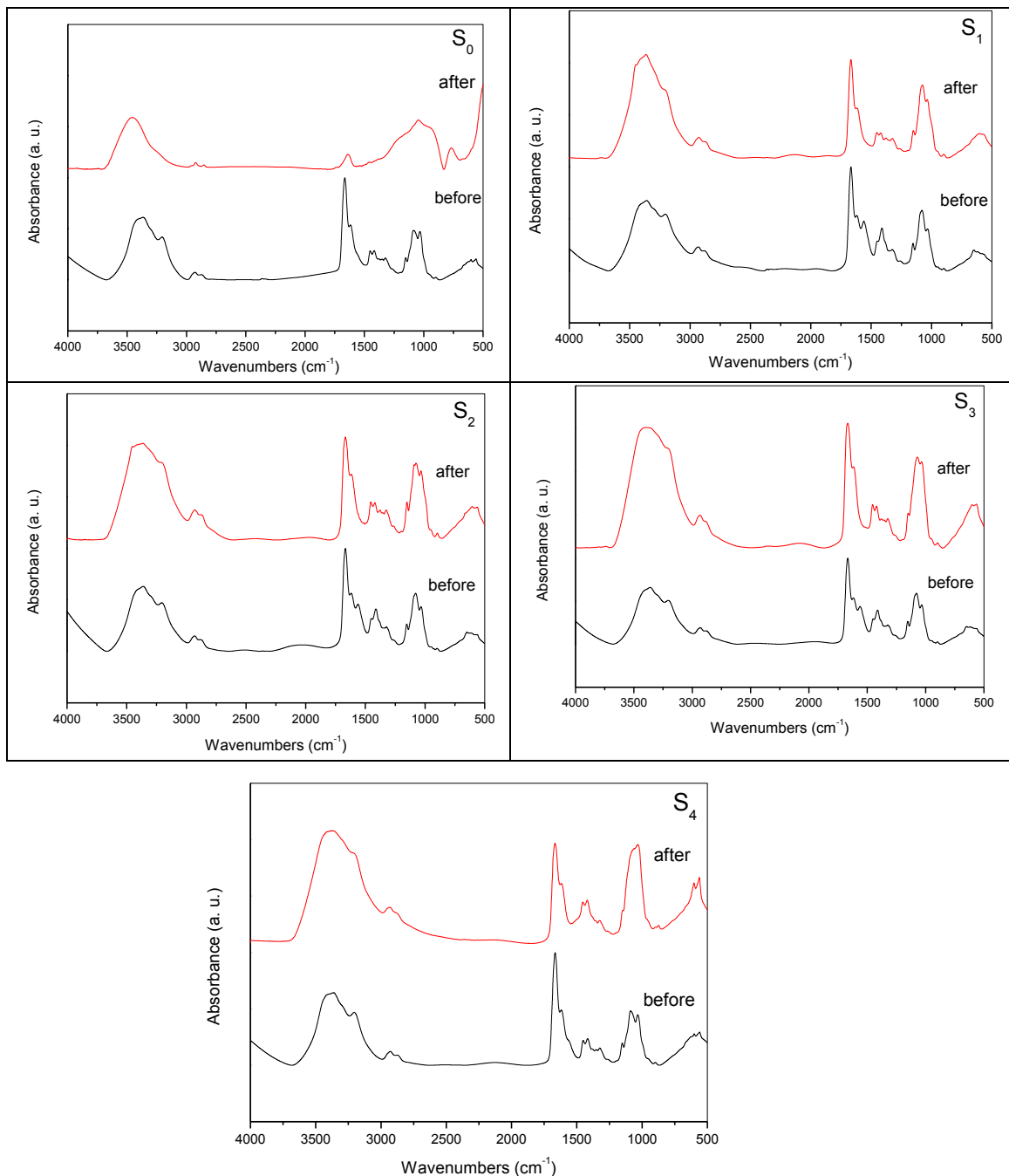


Figure.4. FTIR spectra of HA samples before and after immersion for seven days in SBF.

X-ray powder diffraction (XRD)

Figure.5 shows the XRD pattern of the nano hydroxyapatite product, pure polyacrylamide and pure chitosan. All peaks in the figure corresponding to HA are indexed to hexagonal lattice of crystal. The wide and high peaks reveal that the as-prepared HA has a very small size and excellent crystal quality³ Intensities and lattice parameters for the hexagonal HA are compared with JCPDS card (data file No. 72-1243) standard for HA.

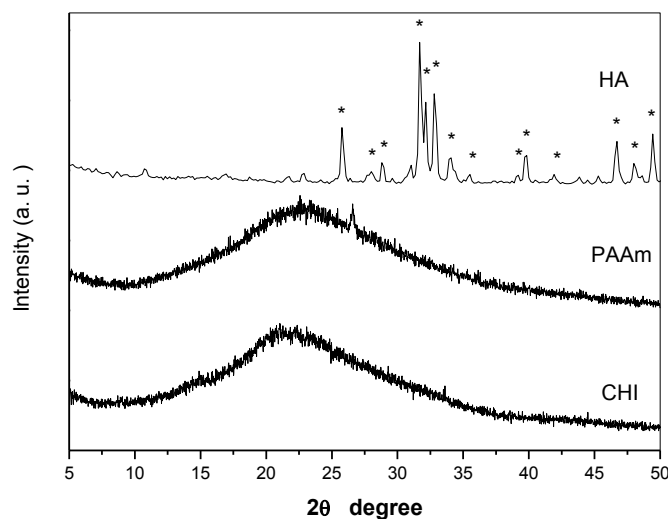


Figure. 5. XRD pattern of prepared Nano hydroxyapatite, pure polyacrylamide and pure chitosan

Figure.6 shows the XRD patterns for blend without and with different concentrations of (1, 2, 5 and 10 wt %) hydroxyapatite. The broad band centered at about 20° was assigned to blend and by increasing HA content this characteristic band became sharper and narrower, implying that the introduction of HA increased the crystallinity of the polymeric matrix.

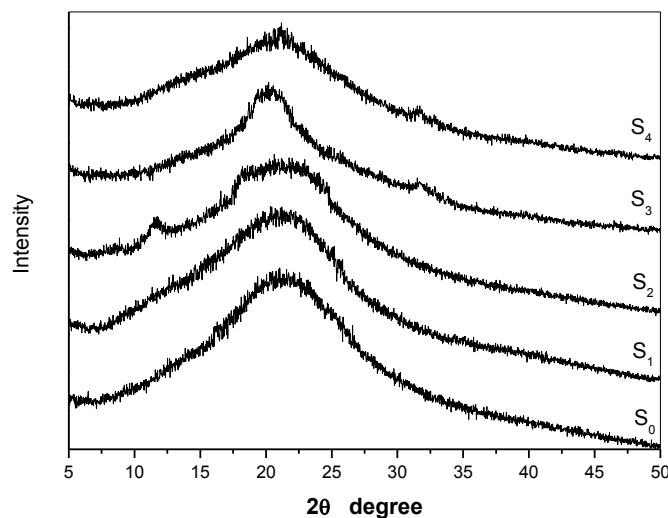


Figure. 6. XRD patterns of blend (50/50) without and with different concentrations of (1, 2, 5 and 10 wt %) hydroxyapatite.

Differential scanning calorimetric (DSC) analysis

It is found from figure .7 that the thermal stability of composites is improved with the increasing of n-HA content. The peaks in case of CHI-PAAm/ HA composites are shifted to higher temperature compared to pure blend, suggestion that the thermal stability of composites is higher than that of pure blend.

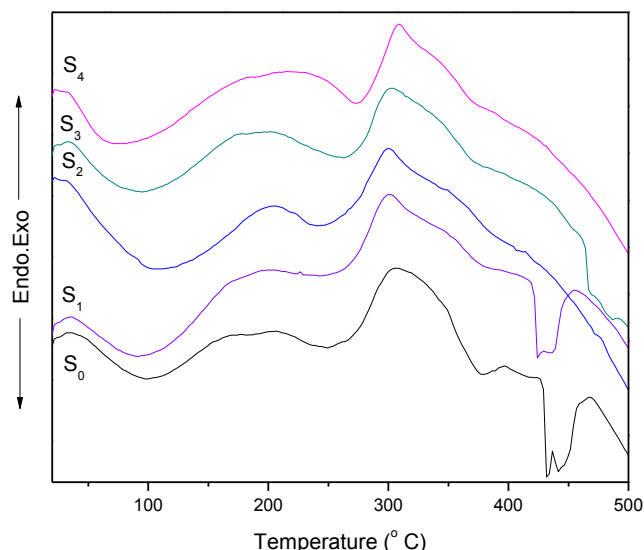


Figure.7.DSC of blend (50/50) without and with different concentrations of (1, 2, 5 and 10 wt %) hydroxyapatite

Transmission electron microscope (TEM)

Figure.8 shows the TEM micrographs of pure HA which indicates that the nano-particles of HA are in the nanometer grad ($15\pm 5\text{nm}$). These results are in good agreement with the micrograph observation in literature^{18, 19}.

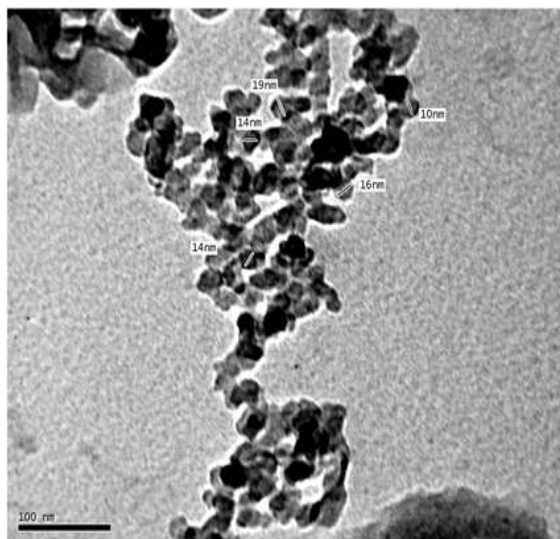


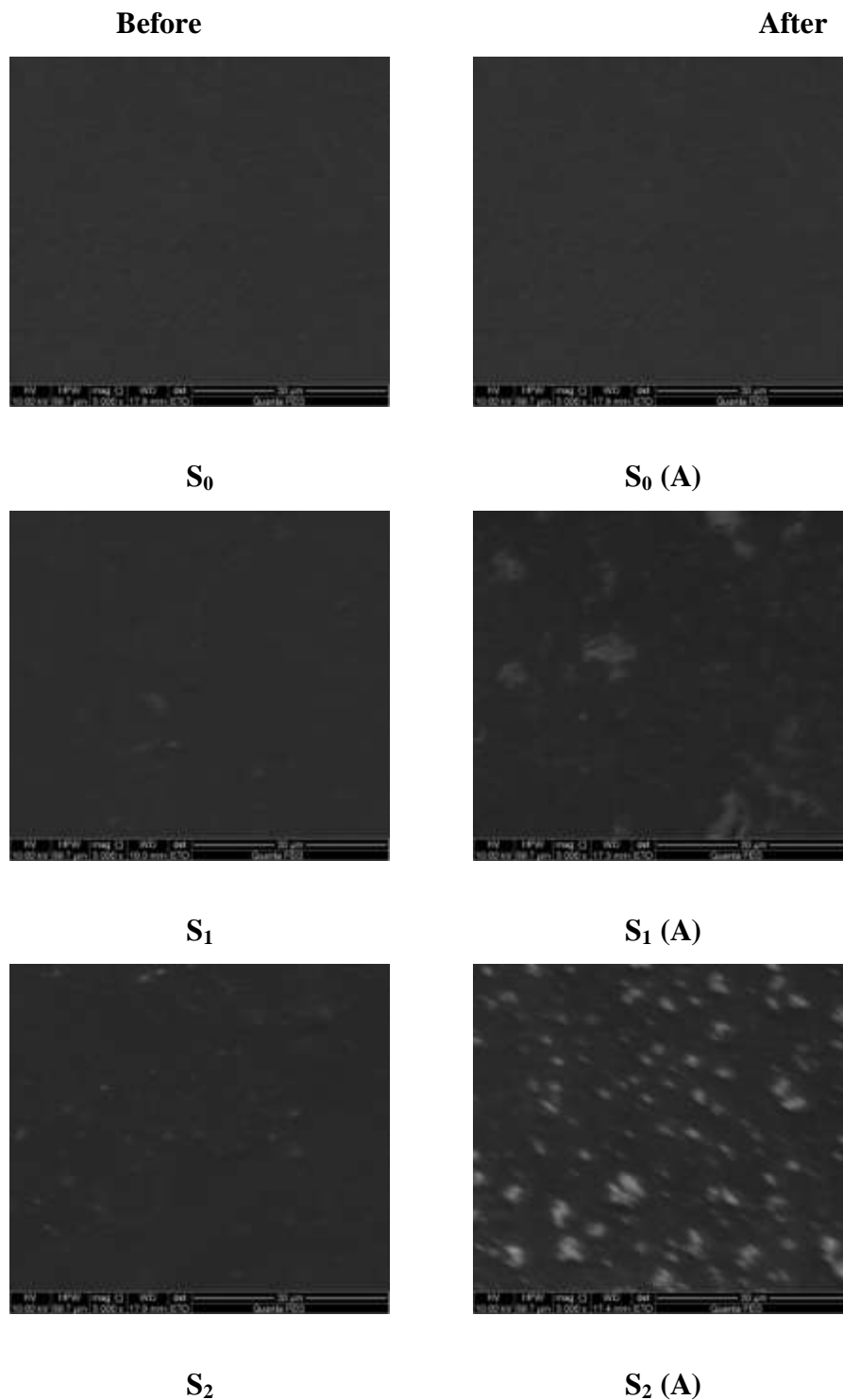
Figure. 8.TEM micrographs for prepared n-HA

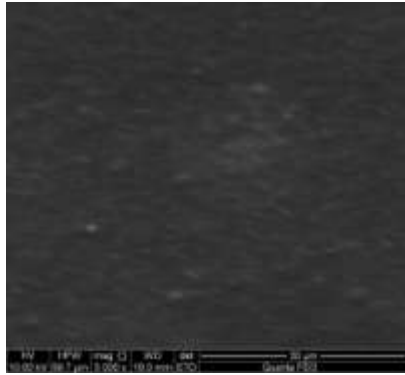
Scanning electron microscopy (SEM)

The SEM images of HA samples before and after immersion for seven days in SBF are shown in figure. 9. SEM of samples before immersion shows few white crystals shapes on the surface of the samples. For seven days after immersion, HA surface has many spherical particles with many pores and some nucleation of particles.

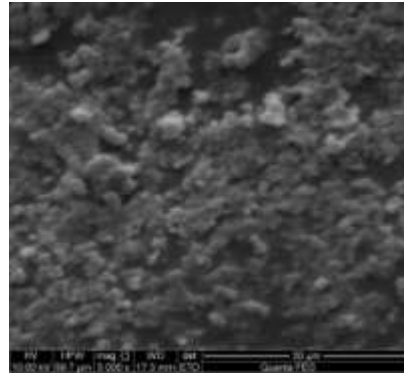
By increasing the concentration more and more apatite particles were deposited, concentrated and covered the surface with many minutes' pores proving effect of immersion.

EDX data showed in Figure. 10 for S₀, S₂, and S₄ samples after immersion in SBF showed that the Ca/P ratio is approximately 1.65, 1.68 and 1.63 for S₀, S₂ and S₄ samples, respectively. It is known that Ca/P ratio in human bone is 1.67²⁰.

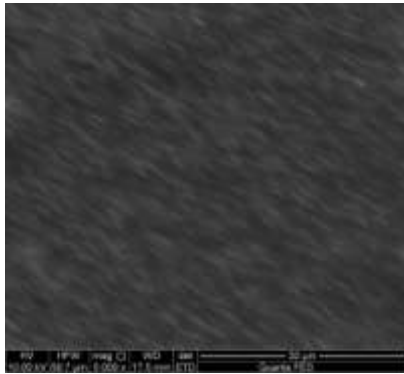




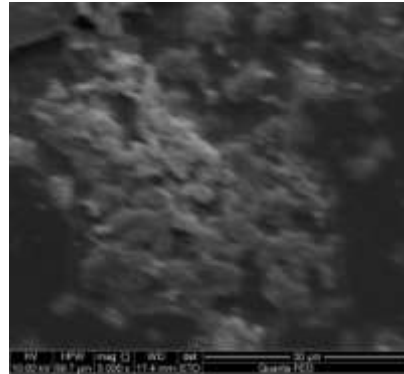
S₃



S₃ (A)

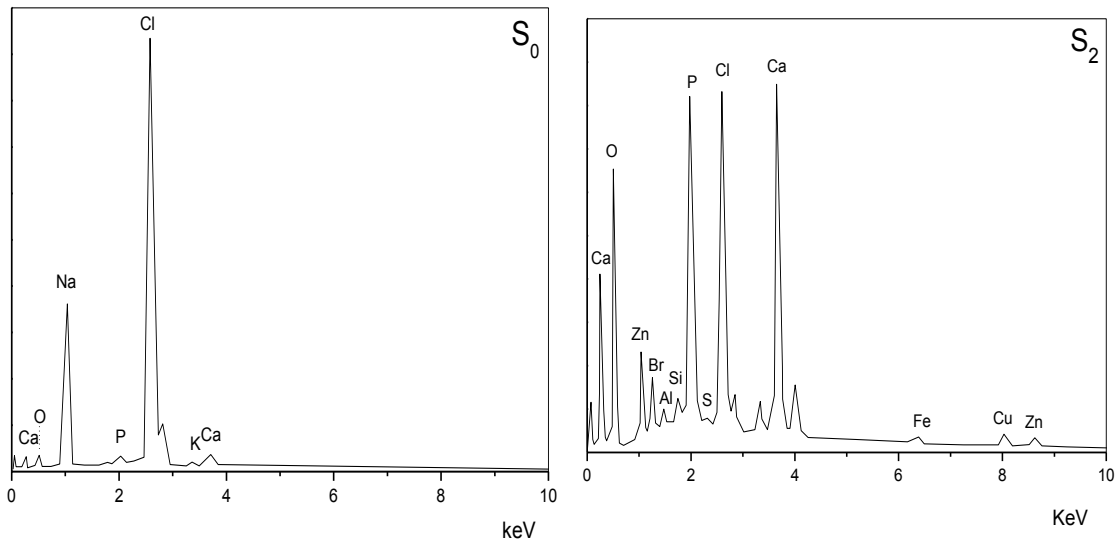


S₄



S₄ (A)

Figure.9. SEM of HA samples before and after immersion for seven days in SBF



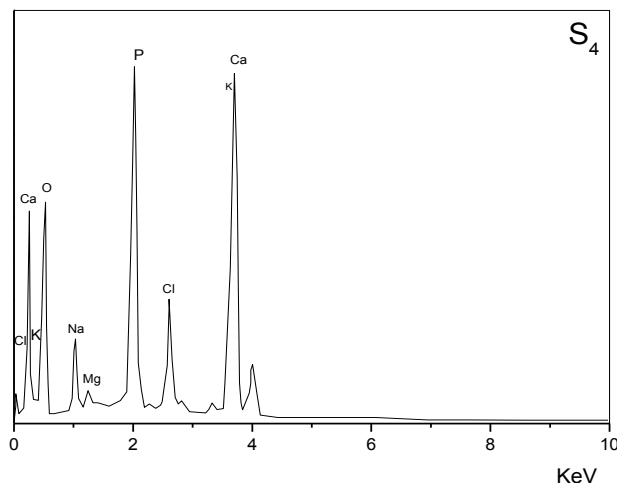


Figure.10.EDX data for S₀, S₂ and S₄ samples after immersion in SBF

CONCLUSION

Chitosan/Polyacrylamide containing nano-hydroxyapatite (HA) composite were prepared via in situ preparation technique. XRD confirm that addition of hydroxyapatite (HA) in the filling level has no effect on the amorphous nature of the base polymeric material with minor change in their crystallinity. FTIR spectra shows maintenance of the basic vibrational band corresponding to chitosan (CHI) and polyacrylamide (PAAm), while the change in the intensity of a peak at 1092 and 1043 cm^{-1} indicates interaction between inorganic and organic matrix and The intensity of HA bands increased after immersion proving that CHI-PAAm polymeric matrix increased the bioactivity of HA due to enhancement of ions deposition on the composite surface and increased by increasing the intensity of HA. Scanning electron micrographs of prepared samples after immersion in (SBF) shows a formation of crystalline regions of HA. So all results indicate that the Chitosan/Polyacrylamide containing nano-hydroxyapatite (HA) composites are the most biocompatible and bioactive materials which can used in biomedical processes.

REFERENCES

1. Eslami H, Solati-Hashjin M, Tahiri M. Synthesis and Characterization of Hydroxyapatite Nanocrystals via Chemical Precipitation Technique. *Iranian Journal of Pharmaceutical Sciences* 2008; 4(2): 127-134.
2. Hule RA, Pochan DJ. Polymer Nanocomposites for Biomedical Applications. *Mrs Bulletin* 2007; 32: 354-358.
3. Liu Y, Hou D, Wang G. Simple wet chemical synthesis and characterization of hydroxyapatite nanorods. *Materials Chemistry and Physics* 2004; 86: 69–73.
4. Ungureanu DN, Angelescu N, Ion RM, Stoian EV, Rizescu CZ. Synthesis and Characterization of Hydroxyapatite Nanopowders by Chemical Precipitation. *International Journal of Biology & Biomedical Engineering* 2011; 5: 57-64.

5. Kalambettu AB, Rajangam P, Dharmalingam S. The effect of chlorotrimethylsilane on bonding of nano hydroxyapatite with a chitosan–polyacrylamide matrix. *Carbohydrate Research* 2012; 352: 143–150.
6. Hui P, Meena SL, Singh G, Agarawal RD, Prakash S. Synthesis of Hydroxyapatite Bio-Ceramic Powder by Hydrothermal Method. *Journal of Minerals & Materials Characterization & Engineering* 2010; 9: 683-692.
7. Sundaram NM, Girija EK, Ashok M, Anee TK, Vani R, Suganthi RV, Yokogawa Y, Kalkura SN. Crystallisation of hydroxyapatite nanocrystals under magnetic field. *Materials Letters* 2006; 60:761–765.
8. Venkateswarlu K, Bose AC, Rameshbabu N. X-ray peak broadening studies of nanocrystalline hydroxyapatite by Williamson–Hall analysis. *Physica B* 2010; 405: 4256–4261.
9. Rehman M, Bonfield W. Characterization of hydroxyapatite and carbonated apatite by photo acoustic FTIR spectroscopy. *Materials in medicine* 1997; 8:1-4.
10. Xiao C, Weng L, Lu Y, Zhang L. Blend Films From Chitosan And Polyacrylamide Solutions. *J. Macromol. Sci. Pure Appl. Chem.* 2001; 8: 761–771.
11. Zakaria Z, Izzah Z, Jawaid M, Hassan A. Effect of degree of deacetylation of chitosan on thermal stability and compatibility of chitosanpolyamide blend. “Chitosan deacetylation,” *BioResources* 2012; 7(4): 5568-5580.
12. Kalambettu AB, Rajangam P, Dharmalingam S. The effect of chlorotrimethylsilane on bonding of nano hydroxyapatite with a chitosan–polyacrylamide matrix. *Carbohydrate Research* 2012;352: 143–150.
13. Trivedi TJ, Rao KS, Kumar A. Facile preparation of agarose–chitosan hybrid materials and nanocomposite ionogels using an ionic liquid via dissolution, regeneration and sol–gel transition. *Green Chem.* 2014; 16: 320–330.
14. Osuna Y, Gregorio-Jauregui K, Gaona-Lozano JG, de la Garza-Rodríguez Ilyna A, Barriga-Castro Saade H, Lopez L. Chitosan-Coated Magnetic Nanoparticles with Low Chitosan Content Prepared in One-Step. *Journal of Nanomaterials* 2012;7.
15. Baybas D, Ulvi Ulusoy. Polyacrylamide–hydroxyapatite composite: Preparation, characterization and adsorptive features for uranium and thorium. *Journal of Solid State Chemistry* 2012; 194: 1-8.
16. Abdelrazek EM, Ibrahim HS. Effect of heparin calcium different concentrations on some physical properties and structure in Polyacrylamide matrix. *Physica B: Condensed Matter* 2010; 405:4339-4343.
17. Sowwan M, Makharza S, Sultan W, Ghabboun J, Abu Teir M, Dweik H. Analysis, characterization and some properties of polyacrylamide-Ni (II) complexes. *International Journal of the Physical Sciences* 2011; 6(27): 6280-6285.
18. Mollazadeh S, Javadpour J, Khavandi A. *Ceramics International* 2007; 33: 1579.

19. Fenglan X, Yubao L, Xiaoming Y, Hongbing L, Li Z. Mater. J. Sci. Mater. Med. 2007; 18: 635.
20. Yusuf PM. Application of Hydroxyapatite in Protein Purification, Bogor, 2008; 60.



AJPHR is
Peer-reviewed
monthly
Rapid publication
Submit your next manuscript at
editor@ajphr.com / editor.ajphr@gmail.com